Received: June 1, 2022. Revised: July 22, 2022.

INASS

International Journal of
Intelligent Engineering & Systems

http://www.inass.org/

Composite Feature Set Based Dental Image Segmentation Framework through Unsupervised Learning

A. Ramana Kumari[1]* S. Nagaraja Rao[2] P. Ramana Reddy[3]

[1]*Department of Electronics and Communication Engineering,*
Jawaharlal Nehru Technological University Anantapur, AP, India
[2]*Department of Electronics and Communication Engineering,*
G. Pulla reddy Engineering College (Autonomous), Kurnool, AP, India
[3]*Department of Electronics and Communication Engineering,*
JNTUA college of Engineering, Anantapur, AP, India
* Corresponding author's Email: ramani.etm@gmail.com

Abstract: Dental X-Ray (DXR) image segmentation has gained a great research interest due to its significance in various dental related applications such as Dental Diseases Detection, Caries detection, etc. This paper proposes a new DXR image segmentation framework based on Adaptive Fuzzy C-Means Clustering which considers not only the gray-level pixel intensities but also the proximity features of dental image such Edges, Boundaries, Color and Binary features. A new background detection mechanism is also proposed to further boost up the segmentation performance. Simulation experiments conducted over a standard DXR image dataset shows the performance effectiveness. Further, the performance of proposed approach is measured through performance metrics such as Specificity, Sensitivity, False Positive Rate, Positive Predictive Value, False Discovery Rate and False Negative Rae proves the outstand performance. The average detection rate of proposed mechanism is observed as 85.21% and the average FPR is observed as 14.79%.

Keywords: Dental image segmentation, Fuzzy c-means clustering, Gradients, Edges, Sensitivity.

1. Introduction

Dental Radiographic Images are the main sources in the dentistry to aid the dental diseases diagnosis. The radiography is an image record produced by passing X-ray signals through an Object. In the case dental radiography, the X-ray is passed through the teeth [1], produces an image representing the structure of teeth.DXR images are generally utilized to analyze the teeth disorder, jaws, structure of bone in the mouth and gums. Without these DXR images, even the dentists could not able to detect the problem until they become severe. In this manner, the DXR images are more helpful for the earlier detection of dental problems thereby a better treatment can be suggested to patient. Forensic identification is one best application of dental images [2]. Generally, these DXR images are helpful in the identification of persons with the help of their DXR images properties. In recent years, the both forensic industry and dentistry are moving towards the automatic methods to analyze the DXR images resulting in a reduced manual burden. Furthermore, with the advancement of pattern recognition algorithms and artificial intelligence, DXR images are being used in an increasing manner to achieve more accurate results with less burden.

Generally, the automatic methods accomplish image segmentation over the images to partition it into several regions of smaller size or into several objects of different properties. In these processes, the Dental Image Segmentation (DIS) is a crucial procedure in real world dentistry to diagnose various dental related diseases. Moreover, it was found that the DIS is an important and necessary step in the analysis of DXR images to get valued and important

data for some medical diagnosis systems and also for some recognition software tools [3]. In earlier, some authors are focused over this aspect and developed various methods to perform the DXR image segmentation. Based on the type of images, the earlier developed works are classified as bitewing X-ray images based approaches [4], periapical dental images based approaches [5] and panoramic dental images based approaches [6]. The bitewing X-ray images and periapical dental images are called as intra-oral images and panoramic dental images are called as extra-oral images. The intra-oral images are acquired inside of the mouth and extra-oral images are acquired from outside of the mouth.

DXR images are pervasively used in the analysis of dental structures. But, due the availability of insufficient resources, DXR image analysis mostly relies on the experience of visual perception of dentist. Moreover, there are so many issues like poor quality of images due to low contrast, noise, region homogeneity between the objects of interest, variations between the teeth of patients, artifacts used for prostheses and restorations, limitation of acquisition methods and space existing by a missing tooth etc., which have a significant effect on the accurate segmentation.

To compensate these issues we develop a novel automatic DXR image segmentation system, the major contributions are highlighted as follows;

- We propose a composite feature extraction method that combines the features of different methods. Instead of single set of features, multiple set of features contribute more towards the segmentation performance.
- We propose an Adaptive Fuzzy C-Means (AFCM) Clustering algorithm to attain an improved segmentation performance at each dental region.
- A new background removal technique is proposed here which is not like a simple thresholding and helps in the perfect segmentation of required regions.
- To validate the proposed approach, it is tested over standard DXR image dataset and evaluated through the metrics like sensitivity, specificity, PPV and FPR.

The further structure of paper is structured as; the discussion about earlier developed DXR image segmentation is done in Section 2. Section 3 completely explores the details of proposed approach of segmentation. Experimental validations and performance analysis are exploredin Section 4 and concluding remarks are providedin Section 5.

2. Literature survey

Due to the significant importance of DXR Image segmentation in the real world dentistry, various methods are developed focusing towards the optimal segmentation performance. Majorly, the DXR gray image consists of two portions, Background portion and Teeth Portion. The Teeth portion is brighter and hence the gray level is high. On the other hand, the background portion is darker and hence it has lower gray levels. Along with these two portions, the dental images also consist of dental structures such as gums, stumps, bones and other periodontitis structures which has medium gray values. The main objective of any segmentation method is to achieve more segmentation performance and it is possible only if the pixels belong to respective portions are clustered correctly.

Depends upon the methodology accomplished for segmentation of dental images, the earlier approaches are broadly classified as Region Based Segmentation Methods, Threshold Based Segmentation Methods, Cluster Based Segmentation methods and Boundary based segmentation methods. In the region based methods, the main objective is to segment the image into various regions and it is done based on the discontinuities in the pixel intensities of image pixels.

Y. Gan et al. [7] proposed a region based segmentation method for the segmentation of tooth and Alveolar bones from dental CT images. Initially, they applied a global convex Level Set (LS) method for the extraction of connected regions of tooth and alveolar bones and then they separated them based on Radon transform and local LS method. However, the LS need considerable through to construct appropriate velocities for advancing the LS function. Moreover, the major issues which are not being solved in LS is the efficiency of signed force, speed function and initial contour segmentation. To solve these problems, A. E. Rad et al. [8] proposed a DXR image segmentation method for caries detection in two phases; Morphological information based IC generation and motion filtering and back propagation algorithm assisted intelligent LS segmentation.

S. Salimzadeh and S. Kandulu [9] proposed teeth segmentation method based on edge lines between crown of teeth. Initially, they processed dental image for pre-processing through Butterworth Low-pass filter and then applied Wavelet transform to determine the directional changes. Then they applied morphological operation to segment the teeth region based on edge lines. S. Datta and N. Chaki [10] applied a marker based watershed

technique to segment the DXR image. They enhanced the Watershed technique by incorporating the marker regions to segment the DXR image properly.

The further class is of threshold based and most of the authors focused on this mechanism only due to its simplicity and ease of accomplishment. In these approaches, the pixels are classified into respective regions based on a pre-determined threshold. Pixels intensities those exceeds the threshold are segmented into one region, while the pixel intensities those are lower than the threshold are segmented into another region. S. Tikhe et al. [11] proposed to detect the enamel caries in interproximal caries through the dental image segmentation. Initially they applied image rotation over input DXR image and then applied histogram analysis to study the intensity level of caries. Next, tooth area is separated through image segmentation and finally the obtained area is processed for identification. J. Mao et al. [12] proposed a full threshold based DXR image segmentation method. Initially, they determined an outline image set and crown image set of the completer target tooth. Then the resultant image's difference is processed for morphological opening. Then the resultant image is subjected to median filtering and the resultant is used as the mask for Grabcut to get the target tooth image.

V. Majanga and S. Virir [13] proposed a Dental image segmentation method based on thresholding and Connected Component analysis (CCA) [14]. They preprocessed the images through Gaussian Blur filter to remove the noise and corrupted pixels. Then the images are enhanced through erosion and dilation based morphology operations. Finally segmentation is done through thresholding and CCA to determine the Region of Interest (ROI). V. Chandran [15] also employed CCA for DXR image segmentation using Otsu's thresholding. At first, they pre-processed the input image for noise and corrupted pixels removal through smoothening filter. Finally, the segmentation is done through Otsu thresholding and CCA to extract the ROI. Compared a single threshold, multiple thresholds will optimize the segmentation performance. Based on this advantage, F. P. Mahdi and S. Kobashi [16] proposed a Quantum Based Particle Swarm Optimization (QPSO) for multi-level image thresholding of DXR images.

The further class is cluster based segmentation. Clustering a method which is used to make the grouping of data automatically based on certain similarity degree in the image. The methodology of clustering depends on the input data and also on the application. The number of groups/clusters to be formulated is the one which has to give as an input to the clustering system. Only limited work is accomplished towards this class in dental images.

M. K. Alsmadi [17] developed an effective, novel and fully automatic panoramic DXR image segmentation model for the jaw lesions. This model applies Fuzzy C-means and Neutrosophic method [18] to segment the jaw image and to detect the jaw lesion region. The obtained results from panoramic X-ray dental images are more helpful in the diagnosis of jaw lesions.

L. H. Son, T. M. and Tuan [19] proposed a new co-operative framework that is based on Semi-supervised Fuzzy Clustering for dental image segmentation. Here the Otsu thresholding is accomplished for the removal of background from an DXR image. Then FCM algorithm is applied to get Dental Structures and finally semi-supervised entropy regularized FCM is applied to improve the segmentation results.

M. Ali et al. [20] proposed a DXR image segmentation algorithm based on fuzzy clustering algorithm and Neutrosophic orthogonal matrices. Initially, the DXR image is transformed into Neutrosophic set and then evaluates the inner products of the cutting matrix of input pixels. Then the pixels are segmented by the orthogonal principles to form clusters. For experimental validation, they used a real dental dataset of Hanoi Medical University Hospital, Vietnam [21].

L. H. Sona et al. [22] proposed a Dental Diagnosis System (DDS) based on segmentation task done through Semi-Supervised Fuzzy Clustering (SSFS). They designed a hybrid system combining the segmentation with classification and decision making. They used a new graph based clustering algorithm called as Affinity Propagation Clustering (APC) for classification. Finally they designed a decision making strategy to determine the final disease from a group of diseases found from the segments.

By incorporating conditional variable into the CSFCM, A.Fariza et al., [23] proposed an extension of CSFCM, called as "Gaussian kernel-based conditional spatial Fuzzy C-Means (GK-csFCM)" to segment the DXR image into four different regions such as Background, Pulp, Dentine and Enamel. CLAHE and Gamma Adjustment are applied for contrast enhancement.

Recently, A. Kumar et al., [24] proposed a semi-supervised fuzzy clustering scheme for dental radiographs segmentation. Initially, the pro-processing is done to minimize the errors. Next, the Otsu thresholding is employed to separate

foreground and background regions. Further a "semi-supervised Hyperbolic Tangent Gaussian Kernel FCM (HTGKFCM)" is employed to get teeth regions.

R. K. Devi et al. [29] proposed a hybrid method for the segmentation of Cyst region from DXR images based on the circularly symmetric isophote properties and Fast marching method (FMM). The Isophote curvature is the curve connecting the pixels with same intensities while the FMM is like a Dijkstra's algorithm and it follows a shortest path from seed area where the information flows outward direction.

Summary of Problem: Most of the above mentioned methods concentrated on the segmentation methodology which can be accomplished through unsupervised learning methods such as K-means and FCM. However, they are generalized methods and not show a significant effect on the DXR segmentation. For an effective DXR image segmentation, the attributes of dental regions must be represented effectively. Even though some authors focused in this direction, they had shown poor performance at the regions where the dental regions have similar pixel intensities. For example, the lower portion of teeth area and dental structures carry similar pixel intensities. In such case, the segmentation method can't perform well and misclassifies the pixels in opposite manner. Due to this reason, the false positive rate of earlier methods is high. To sort out these issues, this work proposes a new method by integrating multiple features to represent the regions in DXR image with effective features. The set of features employed are reverted from multiple attributes like pixel intensities, edge filters, texture features and gradient features. Moreover, our method also contributed at the segmentation by developing a new version of FCM that gets optimized through two sub-objective functions.

3. Proposed approach

In this section, the complete details of proposed methodology are described. Initially, the feature extraction details are discussed and then discusses about the proposed AFCM algorithm. The novelty of this approach is the consideration of different features. Almost all of the conventional approaches accomplished the segmentation algorithms directly over the DXR image whereas this approach initially transforms the input image into a set of features and then FCM is accomplished to group up them into clusters. The detailed methodology of feature extraction and the AFCM is illustrated in the following subsections.

3.1 Feature extraction

In this phase, for every DXR image, totally four set of features are extracted and they are namely, (1) Red-Green-Blue (RGB) features, (2) Pixel Intensity, Edge and Entropy (PEE) Features, (3) Local Binary Pattern (LBP) features, and (4) Gradient Features. The image pixels reveal only limited information about the properties of images. Hence the feature extraction is required through which the segmentation method can gain more knowledge about the properties. In this work, we consider multiple features because the attributes of DXR images are almost have similar pixel intensities. The details of all these feature extraction techniques are described below;

3.1.1. RGB features

The RGB features of an image reveals the color information and these three sets are obtained

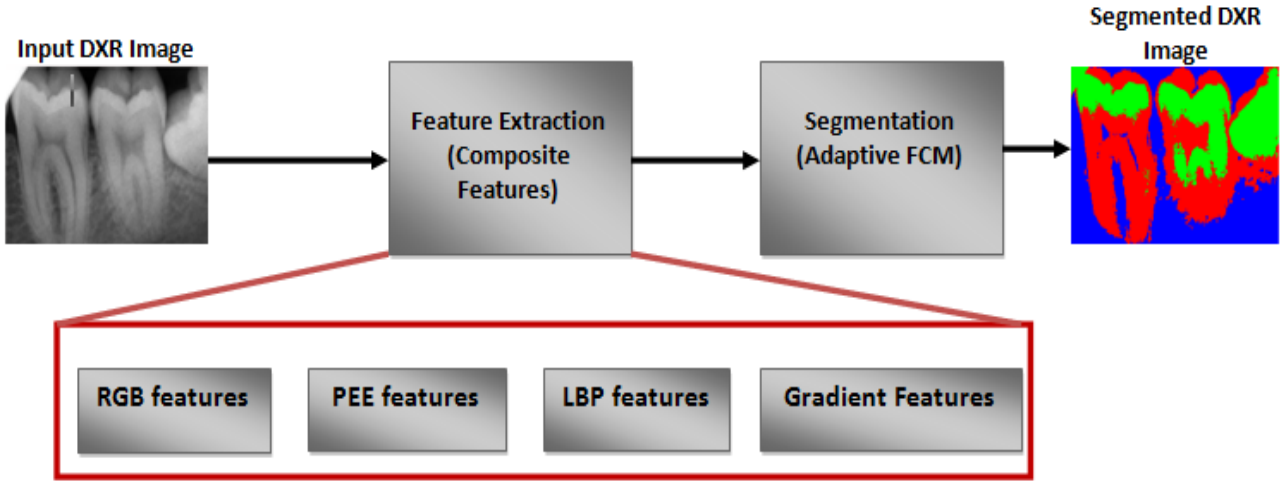

Figure. 1 Overall block diagram of proposed segmentation method

as three planes. For a given color image I, the plane can be I_R, I_G and I_B and can be extracted from the image I as;

$$I_R = I(:,:,1) \rightarrow R - plane \quad (1)$$

$$I_G = I(:,:,2) \rightarrow G - plane \quad (2)$$

$$I_B = I(:,:,3) \rightarrow B - plane \quad (3)$$

Here every pixel of image I is composed of R, G and B, thus the RGB feature (f_{RGB}) is obtained as the average of all planes, as

$$f_{RGB} = \frac{I_R + I_G + I_B}{3} \quad (4)$$

The following Fig. 2 indicates the original color DXR image, and the image with RGB features.

3.1.2. PEE features

Intensity is a normal pixel value and here the intensity feature of a pixel considers its own value along with the intensities of it's neighbor pixels. Simply we can state that the intensity feature of a pixel is formulated as the normalized value of it's adjascent pixels. As shown in Fig. 3 the pixel intensity feature of a pixel located at coordinates *x* and *y* is measured as

$$f_{I(x,y)} = \frac{1}{w^2}\sum_{i=-w}^{w}\sum_{j=-w}^{w} I(i,j) \quad (5)$$

Where w is the size of window/slide and the obatined value is a normalized value of pixel intensities of the neighboring pixels aound the pixel $I(x,y)$. Fig. 3 gives the idea about the pixel intensity feature evaluation.

Next, the Edge feature measures the number of changesin pixel value in a region. The edge feature is extracted from an image as follows;

$$f_{E(x,y)} = \begin{cases} 1, & if\ \nabla f(x,y) \geq T \\ 0, & if\ \nabla f(x,y) < T \end{cases} \quad (6)$$

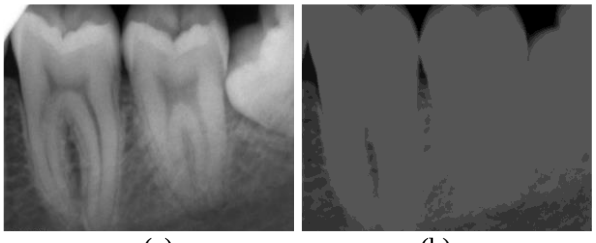

(a) (b)

Figure. 2 RGB featured image results: (a) Color DXR image and (b) RGB featred image

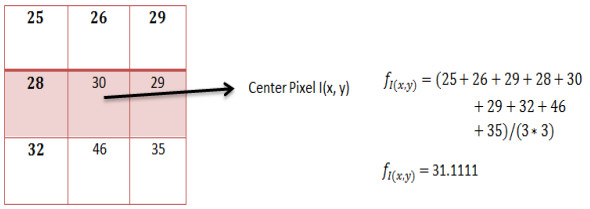

Figure. 3 Pixel inensity feature extraction

Where $\nabla f(x,y)$ is egde strength and it is obatined as

$$\nabla f(x,y) = \sqrt{\left(\frac{\partial I(x,y)}{\partial x}\right)^2 + \left(\frac{\partial I(x,y)}{\partial y}\right)^2} \quad (7)$$

Next, in the PEE meausre, the entropy is calcualted which indicates the randomness of the ifnromation with particular level and is evaluated as follows;

$$r(x,y) = -\sum_{i=1}^{M}\sum_{j=1}^{N} p(x_i,y_j)\log_2 p(x_i,y_j) \quad (8)$$

Where $p(x_i,y_j)$ is the probability pf a pixel located at the coordiantes $x_i, i = 1,2,3,\dots\dots,M$ and $y_j, j = 1,2,3,\dots\dots,N$. Here the M is the row size and N is column size of image and $M * N$ gives the total pixels number present in the image. Further the normalized entropy or entropy feature is evaluated as

$$f_{R(x,y)} = \frac{r(x,y)}{\max\{r(x,y)\}} \quad (9)$$

Where $\max\{r(x,y)\}$ is the maximum entropy value of the given input DXRimage. Here the main intention behind the consideration of PEE features is that they can help in the segmentation of dental structures from background because, the edge values, pixel intensities and entropy values of foreground pixels are too much deviating from the PEE feature of background pixels. Fig. 4 shows the example of PEE featured image.

3.1.3. Local binary pattern (LBP) features

To classify an image through the texture spectrum model, Generally LBP is accomplished.

(a) (b)

Figure. 4 PEE featured image results: (a) Input DXR image and (b) PEE featured image

To ensure a perfect and more discrimination between different objects or regions in the DXR image, LBP features has much appreciable performance and hence this paper considered LBP as one of the feature representations of DXR image. Further the LBP feature also ensures the order of pixel intensities for a given region and the LBP features are considered to be invariant to changes in the illuminations of images. The LBP feature of a pixel located at (x_c, y_c) of a cluster *c* is evaluated as

$$f_{LBP(x,y)} = \sum_{n=0}^{7} s(p_c - p_n)2^n \quad (10)$$

And

$$s(x) = \begin{cases} 1, & x \geq 0 \\ 0, & x < 0 \end{cases} \quad (11)$$

Where p_c is the value of center pixel and p_n is the value of neighbour pixel in the window. A sample representation of an LBP feature of a pixel centered at a window of 3×3 size is shown in the following Fig. 5 and the visual representation of a dental image after the LBP transformation is shown in Fig. 6.

3.1.4. Gradient features

The Gradient features are much useful in the classification of tiny parts of DXR images such as gum, root canal, enamel, and cementum. In the evaluation of gradient features from a DXR image, initially the image was subjected to Gaussian filter to obtain a reduced background noise. Once the Gaussian filtered image is obtained, then it is processed for gradients evaluation through the differences between pixel intensities along horizontal direction and vertical direction. Here every pixel is represented with a gradient vector. Finally a normalized process is applied to obtain a normalized gradient vector for every pixel. The gradient features evaluation is accomplished as follows; For a pixel located at (x, y) in an image *I*, the gradient vector along *x*-direction is measured as

$$g_x(x, y) = (I(x + 1, y) - I(x - 1, y)) \quad (12)$$

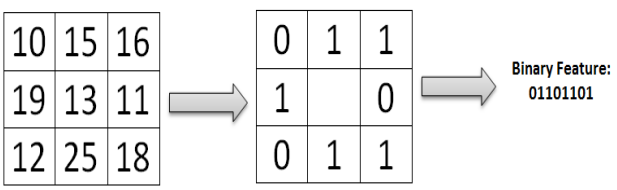

Figure. 5 LBP feature

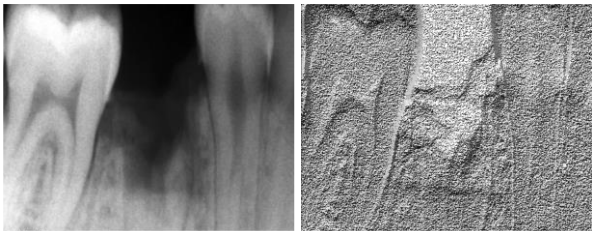

(a) (b)

Figure. 6 LBP featured image results: (a) Input DXR image and (b) LBP featured image

Similarly, the gradient vector along *y*-direction is measured as

$$g_y(x, y) = \big(I(x, y + 1) - I(x, y - 1)\big) \quad (13)$$

Finally, the gradient vector of a pixel $I(x, y)$ is obtained as

$$f_{g(x,y)} = \sqrt{g_x(x, y)^2 + g_y(x, y)^2} \quad (14)$$

Here the gradients are evaluated after smoothing the image through Gaussian filter and it is done as follows;

$$L(x, y, k\sigma) = G(x, y, k\sigma) * I(x, y) \quad (15)$$

Where

$$G(x, y, k\sigma) = \frac{1}{\sqrt{2\pi\sigma^2}} e^{-(x^2+y^2)/2\sigma^2} \quad (16)$$

Where $I(x, y)$ is the pixel vector and $G(x, y, k\sigma)$ is the Gaussian function. Fig. 7 shows the Gradient featured image.

3.2 Segmentation methodology

This section discusses the details of segmentation methodology through the proposed AFCM algorithm. Here the FCM is accomplished in two phases, one phase is through the direct pixel intensities and another is through the extracted features. Simply, the objective function of FCM is

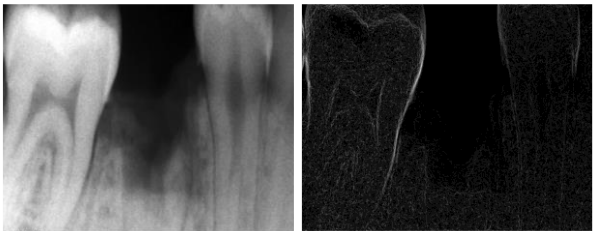

(a) (b)

Figure. 7 Gradient featured image results: (a) Input DXR image and (b) Gradient feared image

formulated as the combination of two sub-objective functions. The first function takes the raw image as input while the second function takes the features as input. The final segmentation considers the minimum value of two sub-objectives, i.e., the cluster with which the convergence is occurred. The pixel is grouped into the corresponding cluster with which it has obtained maximum membership. Further a new measure called Degree of Fuzzy Nearness (DFN) is explained through which the background portions can be removed very effectively. Instead of conventional thresholding techniques like Otsu thresholding, this approach accomplished the degree of fuzzy nearness concept to eliminate the background portions form the DXR image.

3.2.1. Adaptive FCM

The objective function of proposed DXR image segmentation through adaptive FCM is formulated as;

$$J = \min(J_1 + J_2) \tag{17}$$

Here the objective function J is the sum of two sub-objective functions such as J_1 and J_2. Here the first sub-objective J_1 stands for standard functions of FCM and is defined in Eq. (18). This function mainly tries to minimize the distances between cluster center and pixels of the image.

$$J_1 = \sum_{i=1}^{M}\sum_{j=1}^{C} u_{ij}^{m} \left\|X_i - V_j\right\|^2 \tag{18}$$

Where u_{ij} is the membership degree of the pixel X_i with the *j*th cluster and here the cluster center of *j*th cluster is represented as V_j; m denotes the level of fuzziness and it is generally set to 2. This algorithm assigns one membership value for every pixel based on the Euclidean distance between the corresponding pixel and cluster centers. The higher membership value denotes that the pixel is more nearer to the cluster center and lesser value denotes that the pixel is farer to the cluster center. The membership function is evaluated accordingly as

$$u_{ij} = 1/\left(\sum_{k=1}^{C}\left(\frac{d_{ij}}{d_{ik}}\right)^{\left(\frac{2}{m-1}\right)}\right) \tag{19}$$

And the cluster center is mathematically formulated as

$$V_j = \left(\sum_{i=1}^{M}(u_{ij}^{m})x_i\right)/\left(\sum_{i=1}^{M}(u_{ij}^{m})\right), \quad \forall\, j = 1,2,3,\ldots,C \tag{20}$$

Where M is the total pixels count present in the DXR image and the term $\left\|X_i - V_j\right\|$ denotes the Euclidean distance between *i*th pixel and *j*th cluster center.

Further towards the second objective J_2, this paper proposed an adaptive sliding window to find out the neighbor pixels for a given pixel. Due to the high correlations between the pixels of image, two neighbor regions have an analogous value. For a given two pixels, the distance will declare whether they belong to same cluster or not. If the distance between two neighbor pixels is greater than a particular threshold, then those two pixels are said to be different and belongs to different clusters. Similarly, if the distance between two pixels is less than the threshold, then they are said to be same and belongs to same cluster.

Here the proposed sliding window captures the range, i.e., upto what size of extent the pixels around it are analogous to it. To find out those pixels, the proposed approach accomplished the sliding window of size starting form 3*3. For every phase of slide, the center pixel is compared with the mean of its neighbor pixels in the window. If the difference is observed as smaller than a threshold, the size of sliding window is increased by a unit in all directions. If the difference is observed as larger than the threshold, then record that as final optimal size. Let's consider *w* is the optimal size of sliding window, and then a new factor called distance membership function (DMF) is defined as

$$DMF_{ik} = \frac{\sum_{j=1}^{w} u_{ij}\left(\frac{1}{d_{kj}}\right)}{\sum_{j=1}^{w}\left(\frac{1}{d_{kj}}\right)} \tag{21}$$

Where u_{ij} is the degree of membership between the *i*th pixel to the *j*th cluster and the term d_{kj} is the squared Euclidean distance between the pixel (x_k, y_k) and the cluster center (x_j, y_j). The main objective of this function is to calculate the distance membership relation between the *k*th pixel to the *j*th cluster. Form this DMF a new fuzzy distance is evaluated as

$$Q_{ik} = \|X_k - V_i\|^2(1 - \alpha e^{-DMF_{ik}}) \tag{22}$$

Where $\alpha \in [0\ 1]$ is an arbitrary constant which controls the fuzzy distance. For an $\alpha = 0$, the expression in Eq. (22) becomes a normal Euclidean distance between *k*th pixel and *i*th cluster. Next to achieve the main objective of FCM, i.e., minimization of fuzzy distance between pixels and

cluster centers, the first sub-sub-objective of sub-objective J_2 is formulated as

$$J_{21} = \sum_{i=1}^{M} \sum_{j=1}^{C} u_{ij}^{m} \, Q_{ji}^{2} \tag{23}$$

Further the second sub-sub-objective of sub-objective J_2 is formulated as

$$J_{22} = \sum_{i=1}^{M} \sum_{j=1}^{C} u_{ij}^{m} \left(\frac{1}{l} \sum_{i=1}^{l} f_l \right) \tag{24}$$

Where f_l $(l = 1, \ldots\ldots, 4)$ are the normalized features extracted from the original DXR image, as discussed in the section III.A. Finally the second sub-objective is obtained as

$$J_2 = J_{21} + J_{22} \tag{25}$$

3.2.2. Degree of fuzzy nearness (DFN)

Here the DFN improvises the segmentation performance by removing the background pixels from the image very effectively. The concept of DFN is initially discovered by Wang [26]to measure the similarity between fuzzy sets.

The axiomatic demonstration of DFN is given according to the following definitions;
If the mappingfunction $d: F(X) \times F(Y) \rightarrow [0\ 1]$,
$\forall\ A, B, C \in F(X)$, satisfies the below rules;
(1) $d(A, A) = 1$
(2) $d(A, B) = d(B, A)$
(3) $A \subseteq B \subseteq C \Longrightarrow d(A, C) \leq d(A, C) \wedge d(A, B)$

Here the d is termed asDFN of function F(X) and the term $d(A, B)$ denotes the DFN between two fuzzy sets A and B. There are so many ways to define the degree but this paper considered the arithmetic mean and is formulated as

$$d(A, B) = \frac{2 \sum_{k=1}^{N} A(x_k) * B(x_k)}{\sum_{k=1}^{N} A(x_k) + B(x_k)} \tag{26}$$

The above mentioned functions explore the connectivity between background and teeth regions. For a given region, if the pixel belongs to same region, then the harmonic mean is same (according to mapping function 1). Next, if the DFN of a pixel in two sets A and B is *d(A,B)*, then the DFN of same pixel in the same two sets B and A is same, because the pixel intensity is same. In the proposed background detection, the degree d is used to measure the DFN between two factors such as fuzzy background vector H and fuzzy membership degree vector u_{ij}. Then it was employed to measure the pixel's belongingness to either teeth region or background region and it is obtained through the following mathematical formulation.

$$F(X) = \begin{cases} 1, & d(H, u_{ij}) < T \\ 0, & d(H, u_{ij}) \geq T \end{cases} \tag{27}$$

Where T is a threshold. Based on Eq. (27) the pixel is classified as foreground/teeth region if $F(X)$ is equal to 1 or background if $F(X)$ is equal to 0. This DFN is accomplished at the starting of segmentation methodology. It is applied after the accomplishment of FCM (fist objective J_1) to efficiently separate the pixels into the teeth regions and background regions. Further the foreground areas/regions are processed for further segmentation into teeth area, dental structures such as bones, gums and some other structures.

4. Results and discussion

This section discusses the particulars of experiments carried out over the proposed segmentation mechanism. Initially the details about the database procurement are discussed and then the segmentation results obtained after the accomplishment of proposed method over the database images is discussed. Finally the performance is analyzed through several metrics.

4.1 Database details

The DXR image database [27] considered for simulation experiments are grayscale images and size of every test image is 748*512. In every image, the last twelve rows contain the information of images in which the abnormality is specified by the medical expert. All the images are in the '.jpeg' format. These images are already assessed by human medical professionals to certify that all the DXR images are appropriate for analysis. Fig. 8 shows some examples of test images considered for simulation.

4.2 Results

The proposed segmentation mechanims is tested approximately over 75 images. For every image, the propsoed approach tries to extarct three regions namely, teeth area, dental strcutures, and background. In every output, the images are color coded with different colours. Each region is represented with one color. According to the theoritical discussion if we consider DXR image, visually it looks like a gray scale image and it consists of only teeth regions and background

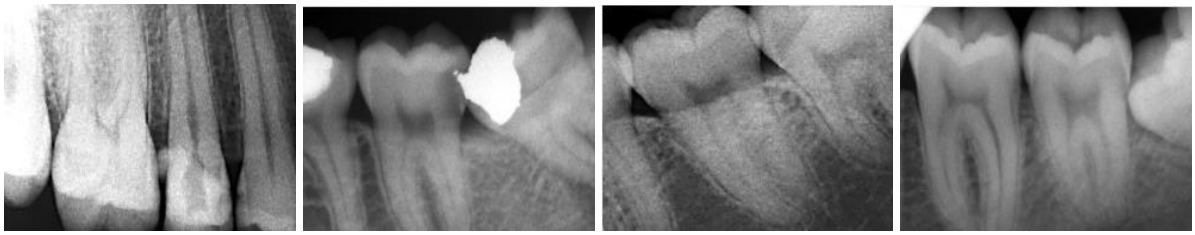

Figure. 8 Test images cosnidered for simulation experiments

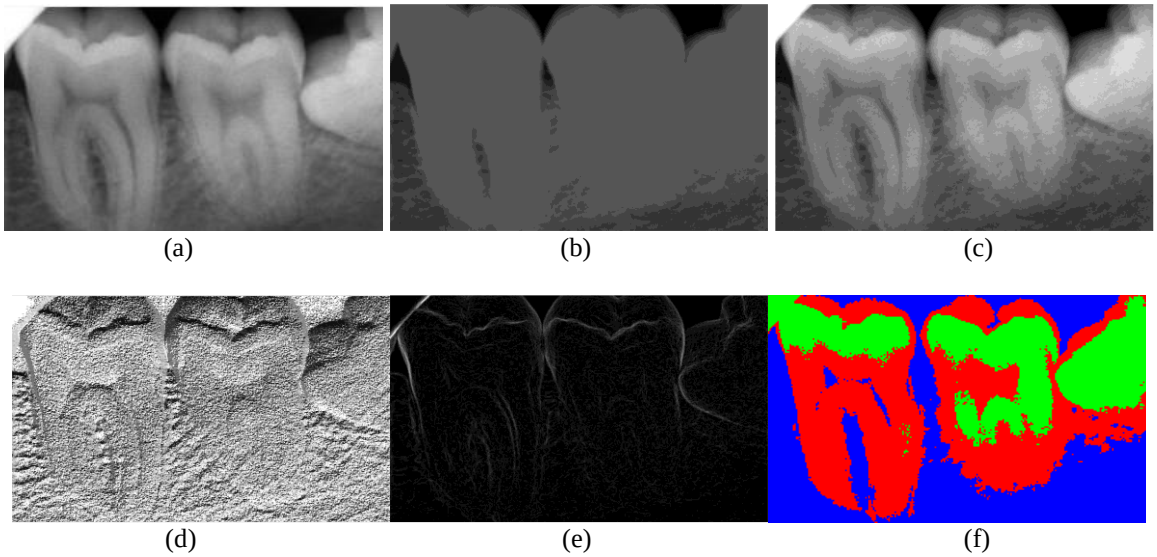

Figure. 9 Results of proposed segmentation method: (a) Original DXR image, (b) RGB featured image, (c) PEE featured image, (d) LBP featured image, (e) Gradient featured image, and (f) Segmented image

regions. Further in the teeth regions, this proposed approach tried to separate the dental structures such as gums, bones, and some other stcuctures for teeth region. Some Example output images are shown in Fig. 9.

As shown in the Fig. 9, the segmented images are color coded and each color represents one region. Here the Red Color region represents the teeth area, green color represents the dental structures and the blue color is allocated for background representation. Fig. 9 (a) represents the original DXR images, Fig. 9 (b) represents the RGB featured image. The RGB featured image is obtained after the accomplishment of RGB feature extraction method over the original image. Further feature is PEE and the obtained PEE featured images are shown in Fig. 9 (c). Next, the Fig. 9 (d) and 9 (e) represents the LBP featured images and Gradient featured images respectively. Once the features are extracted from input test images, the proposed AFCM is applied over it to segment the individual regions such as teeth region, dental structures and background. The obtained segmented results are depicted in Fig. 9 (f). Due to the non-constant variations in the grey-levels of image, the dental image segmentation is tough. To solve this problem, the proposed approach not only considered the grey-level pixel intensities but also the extra features such as RGB features, PEE features, LBP features, and Gradient features. Each feature has its own significance in the provision of a perfect clarity to the segmentation mechanism towards the dental structures.

4.3 Performance analysis

The results shown in the above sub-section reveals the performance effectiveness through the visual analysis. Further, for quantitative assessment, we referred some secondary measures like False Negative (FN), False Positive (FP), True Negative (TN) and True Positive (TP). Based on these measures, the primary measures are calculated. The primary measures are namely True Positive Rate (Sensitivity), Positive Predictive Value (PPV), Specificity, False Positive Rate (FPR), False Negative Rate (FNR) and False Discovery Rate (FDR) and they are represented according to Eqs. (28) to (33) respectively.

$$Sensitivity\ or\ True\ Positive\ Rate\ (TPR) = \frac{TP}{TP+FN} \times 100 \quad (28)$$

Sensitivity measures the quantity of positives that are appropriately identified as such.

$$Specificity\ or\ True\ Negative\ Rate\ (TNR) = \frac{TN}{TN+FP} \times 100 \quad (29)$$

Specificity measures the quantity of negatives that are appropriately identified as such.

$$Positive\ Predictive\ Value\ (PPV) or\ Precision = \frac{TP}{TP+FP} \quad (30)$$

Precision measures the quantity of Positives that is appropriately identified in the presence of other.

$$False\ Positive\ Rate\ (FPR)\ or\ Fall-out = \frac{FP}{TN+FP} \times 100 \quad (or)\ \ 1 - TNR \quad (31)$$

Fall-out measures the quantity of Positives that are incorrectly identified in the presence of other.

$$False\ Negatve\ Rate\ (FNR)\ or\ Miss\ rate = \frac{FN}{FN+TP} \times 100 \quad (or)\ \ 1 - TPR \quad (32)$$

Miss rate measures the quantity of negatives that are incorrectly identified in the presence of such.

$$False\ Discovery\ Rate\ (FDR) = \frac{FP}{FP+TP} \times 100 \quad (or)\ \ 1 - PPV \quad (33)$$

FDR measures the portion of positives that are incorrectly classified in the presence of other.

The proposed approach was tested approximately over 75dental X-ray image samples and the obtained Sensitivity, Specificity, PPV and FPR, FNR and FDRare shown in the following Table 1. After the segmentation, the pixels of ground truth image is compared with the pixels in the segmented image. If the category of a pixel in ground truth and segmented image are same, then it is considered as TP, otherwise it is FN. The obtained TPs, FNs, and FPs are substituted in the above equations to get TPR, TNR etc. This process is applied for all pixels of given input image and the obtained average values are depicted in Table. 1. Due to the space limitation, the Table. 1 depicts the results of only twenty images and the average results are represented in the further figures.

Further to explore the performance of proposed method, the segmnetation results such as TPR, TNR, PPV, and FPR are comapred with the resuls of conventional approaches such as Teeth Segmentation of DXR images using Gaussin Kernel Spatil FCM (GKSFCM) [23], Thresholding and CCA (T_CCA)[13] and Hybrid Fuzzy C-means Algorithm (HFCM) [17]. The thresholding and CCA is the very traditional method which applies mathematical morphology to find out the connected pixles in the image. However, it is insufficinet when the image is contaminated with noise as the addition of noise makes the pixel to change. In such condition, the CCA shows much poor perfromance.

Table. 1 Segmentation performance of proposed approach

ImageSample	Sensitivity (TPR)	Specificity (TNR)	Precision (PPV)	Fall-out (FPR)	Miss rate (FNR)	FDR
Sample 1	0.8523	0.8244	0.8620	0.1756	0.1477	0.1380
Sample 2	0.8325	0.8046	0.8422	0.1954	0.1675	0.1578
Sample3	0.8641	0.8362	0.8738	0.1638	0.1359	0.1262
Sample4	0.8247	0.7968	0.8344	0.2032	0.1753	0.1656
Sample5	0.8542	0.8263	0.8639	0.1737	0.1458	0.1361
Sample6	0.7958	0.7679	0.8055	0.2321	0.2042	0.1945
Sample7	0.8006	0.7727	0.8103	0.2273	0.1994	0.1897
Sample8	0.8347	0.8068	0.8444	0.1932	0.1653	0.1556
Sample9	0.7769	0.7490	0.7866	0.2510	0.2231	0.2134
Sample10	0.8396	0.8117	0.8493	0.1883	0.1604	0.1507
Sample11	0.7834	0.7555	0.7931	0.2445	0.2166	0.2069
Sample12	0.8637	0.8358	0.8734	0.1642	0.1363	0.1266
Sample13	0.7958	0.7679	0.8055	0.2321	0.2042	0.1945
Sample14	0.8444	0.8165	0.8541	0.1835	0.1556	0.1459
Sample15	**0.8745**	**0.8466**	**0.8842**	**0.1534**	**0.1255**	**0.1158**
Sample16	0.8597	0.8318	0.8694	0.1682	0.1403	0.1306
Sample17	0.7679	0.7405	0.7776	0.2595	0.2321	0.2224
Sample18	0.8029	0.7750	0.8126	0.2250	0.1971	0.1874
Sample19	0.8647	0.8368	0.8744	0.1632	0.1353	0.1256
Sample20	0.7863	0.7584	0.7960	0.2416	0.2137	0.2040

Next, HFCM is a Clustering technique which applied the traditiaonl FCM for custering the DXR image several regions. However, it considered only pixel intensities as a reference to cluster the entire image which is insufficient to discriminate similar dental regions. The recent GKSFCM discriminated between noise and dental pixels correctly by computing the Gaussin distribution. However, it also cosnidered only pixel intensities as a reference for segmentation. Unlike all the methods, our method employed a pixel level clasisifcation which segments each pixel into the corresponding segment. The proposed method is novel since it represented each pixel with a set of features which explores the characteristics of pixels in multiple domains. These characteristics help in the identification of pixels perfectly even under worst conditions.

Here the comparitive analysis is accomplished in two phases, one is before enhancement and another is after enhancement. In the former case, the DXR image is directly processed for segmentation while in second case the DXR image is initially subjected to contrast enhancement through the method proposed in [28] and then subjected to segmentation through proposed approach. Fig. 10 to 15 demonstrates the comparitive analysis between the proposed and several existing methods.

Sensitivity reflects the capability of a method in the determination of exact values. Here, the Sensitivity is defined with respect to the segmentation of regions (pixels classification into the correct regions). The sensitivity plot for the developed mechanism and existing methods is demonstrated in Fig. 10. From the figure, the sensitivity of proposed approach is observed as high compared to conventional approaches, thus the proposed can efficiently segments the teeth and teeth related regions from background. On an average, the TPR of developed mechanism before enhancing the DXR image is obtained as 0.7814 whereas it is of 0.7777, 0.7749 and 0.6523 for GKSFCM, HFCM and Thresholding with T_CCA respectively. After enhancing and testing the DXR image, the obtained sensitivity is observed as 0.8753, 0.8685, 0.8643, and 0.8023 of Proposed, GKSFMC, HFCM and TSMM respectively.

Next, Fig. 11 shows the results comparison with respect to the specificity which signifies the effectiveness in the segmentation of other than teeth related regions. Higher value of specificity shows the better performance and vice versa. As it can be observed, the specificity of developed mechanism is better than the existing methods. Since the developed mechanism accomplished a two phase optimization through FCM, all the regions are

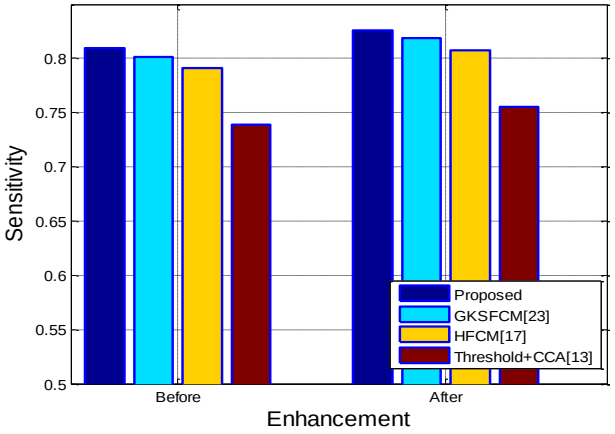

Figure. 10 Sesnitivity comparison before and after enhancement

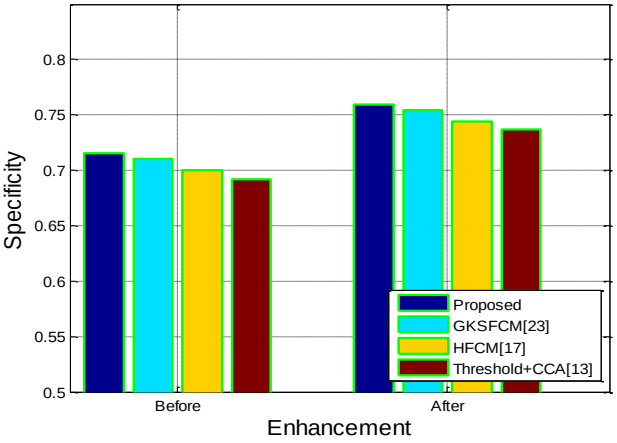

Figure. 11 Specificity comparison before and after enhancement

perfectly segmented. Further, due to the accomplishment of four different features for every pixel of image, the clustering algorithm achieve perfect differentiation between the regions and thus resulted in a greater sensitivity and specificity. On an average, the specificity of proposed approach before enhancing the DXR image is obtained as 0.7140 whereas it is of 0.7122, 0.7114 and 0.6524 for GKSFCM, HFCM and T_CCA respectively. After enhancing and testing the dental X-ray image, the obtained specificity is observed as 0.7383, 0.7362, 0.7358, and 0.6585 of Proposed, GKSFCM, HFCM and T_CCA respectively.

PPV also observed as more for the proposed approach than the conventional approaches. PPV signifies the nature of proposed system in the precise detection. As much as high PPV, the regions are said to be segmented more precisely, i.e., the pixels belong to teeth region are clustered into teeth regions only. Precision comparison is shown in Fig. 12. On an average, the PPV of proposed approach before enhancing the DXR image is obtained as 0.7427 whereas it is of 0.7409, 0.7392 and 0.6966

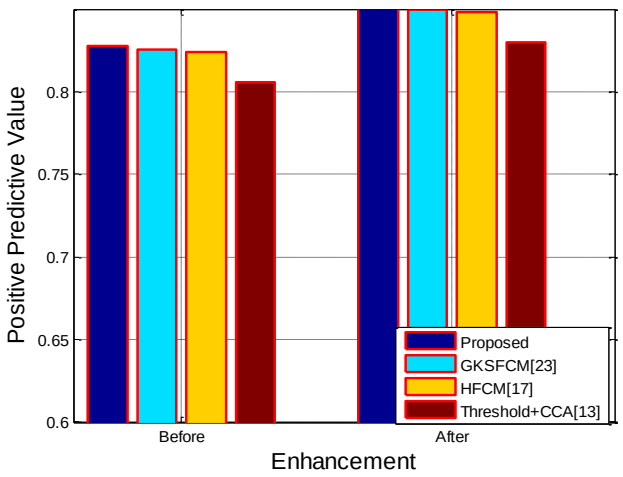

Figure. 12 PPV comparison before and after enhancement

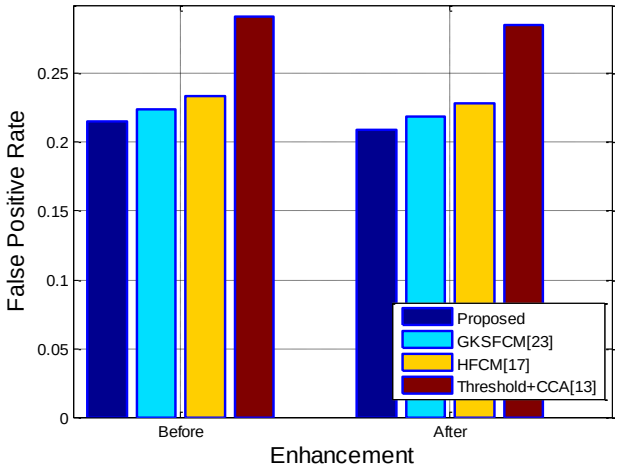

Figure. 13 FPR comparison before and after enhancement

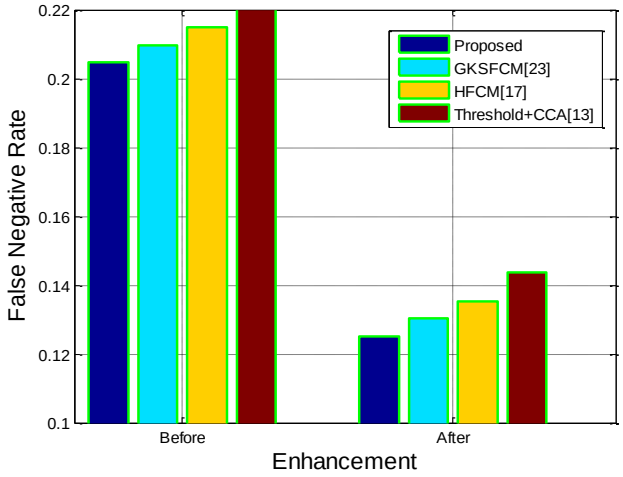

Figure. 14 FNR comparison before and after enhancement

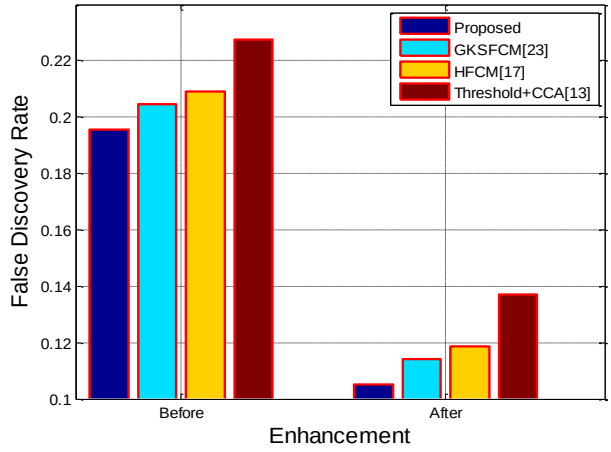

Figure. 15 FDR comparison before and after enhancement

for GKSFCM, HFCM and T_CCA respectively. After enhancing and testing the DXR image, the obtained PPV is observed as 0.7678, 0.7655, 0.7643, and 0.7103 of Proposed, GKSFCM, HFCM and T_CCA respectively.

The FPR is metric which defines the false positives, i.e., the pixel counts which were clustered into one region but belongs to another region. For instance, if one pixel belongs to teeth region is labeled as dental structure after the accomplishment of clustering over it, then it is considered as false positive. An Accumulated count of such pixel count is divided with total number of pixel and is called as FPR. FPR measure the number of pixels which are misclassified. The FPR comparison is shown in Fig. 13 and it can be observed that the proposed approach has less FPR than the conventional approaches. On an average, the FPR of proposed approach before the enhancement of DXR is obtained as 0.2095 whereas it is of 0.2122, 0.2263 and 0.2729 for GKSFCM, HFCM and T_CCA respectively. After enhancing and testing the DXR image, the obtained FPR is observed as 0.2003, 0.2198, 0.2241, and 0.2567 of Proposed, GKSFCM, HFCM and T_CCA respectively.

FNR is measured as the count which was classified as false for a given negative input. For example, if the pixel belongs to Background region is clustered into the region belongs to teeth region, it is considered as FN. An Accumulated count of such pixels is divided with total number of pixels is called as FNR and the comparison is shown in Fig. 14. From the results, the FNR of developed mechanism is less compared to the existing methods due to the four stage feature representation and Adaptive clustering. On an average, the FNR of developed method before the enhancement of DXR is obtained as 0.2025 whereas it is of 0.2096, 0.2100 and 0.2193 for GKSFMC, HFCM and T-CCA respectively. After enhancing and testing the DXR image, the FNR is observed as 0.1256, 0.1309, 0.1357, and 0.1432 of Proposed, GKSFCM, HFCM and T_CCA respectively.

The final performance metric, FDR is compared and the results are shown in Fig. 15. FDR is

opposite of PPV, means it measures the total pixel's count those are not precisely classified. A larger value of FDR signifies the lesser performance and vice versa. On an average, the FDR of developed mechanism before the enhancement of DXR image is obtained as 0.1950 whereas it is of 0.2050, 0.2100 and 0.2280 for GKSFCM, HFCM and T_CCA respectively. After enhancing the obtained FDR is observed as 0.1080, 0.1125, 0.1198, and 0.1345 of Proposed, GKSFCM, HFCM and TSMM respectively.

5. Conclusion

This paper proposed a novel DXR image segmentation mechanism based on the AFCM and effective feature extarction process. The proposed feature extraction process is very much helpful for FCM in segmenting the regions more accrately. Further the two phase FCM also shown it's contribution in acheveing a gretaer performance in the dental regions segmentation. The experimental results over the standard DXR image dataset designate theability of the developed method in segmenting dental images. As a performance evaluation metrics, the proposed approach evaluated TPR, TNR, PPV and FPR to show the performance assessment. Further the comparative analysis done between the developed and several existing methods has shown the performance improvement from the conventional approaches in achieving the better segmentation performance. From the segmentation results, it is observed that, on an average, the TPR of Developed mechanism is obtained as 0.8233 whereas it is of 0.8163 and 0.8074 for HFCM and TSMM respectively. Further the average FPR is observed as 0.2438, 0.2452, and 0.2467 of proposed, HFCM and TSMM respectively.

Conflicts of interest

This research work is not supported by any financial support. The authors did not receive financial support from any organization for the submitted work. The authors won't have any conflict of interests.

Author contributions

A. Ramana Kumari contributed towards the design and development of the main proposed method of this paper.

S. Nagaraja Rao and P. Ramana Reddy contributed towards the guidance and verification of experimental validation respectively.

References

[1] R. A. Quinn and C. C. Sigl, "Radiography in Modern Industry", *4th Edition, New York, Eastman Kodak Company*, 1980.

[2] E. Paewinsky, H. Pfeier, and B. Brinkmann, "Quantification of secondary dentine formation from orthopantomograms: a contribution to forensic age estimation methods in adults", *Intl. Journal of Legal Medicine*, Vol. 119, No. 1, pp. 27-30, 2005.

[3] A. D. Association, "Dental radiographic examinations – recommendations for patient selection and limiting radiation exposure", *Journal of the American Medical Association*, Vol. 25, No. 14, pp. 1929-1936, 1987.

[4] C. W. Wang, C. T. Huang, J. H. Lee, C. H. Li, S. W. Chang, M. J. Siao, T. M. Lai, B. Ibragimov, T. Vrtovec, O. Ronneberger, P. Fischer, T. F. Cootes, and C. Lindner, "A benchmark for comparison of dental radiography analysis algorithms", *Medical Image Analysis*, Vol. 31, pp. 31:63-76, 2016.

[5] S. S. Dighe and Revati, "Preprocessing, Segmentation and Matching of Dental Radiographs used in Dental Biometrics", *International Journal of Science and Applied Information Technology*, Vol. 1, No. 2278, pp. 52-56, 2012.

[6] Y. Y. Amer and M. J. Aqel, "An efficient segmentation algorithm for panoramic dental images", *Procedia Computer Science*, Vol. 65, pp. 718-725, 2015.

[7] Y. Gan, Z. Xia, J. Xiong, G. Li, and Q. Zhao, "Tooth and Alveolar Bone Segmentation From Dental Computed Tomography Images", *IEEE Journal of Biomedical and Health Informatics*, Vol. 22, No. 1, pp. 196-204, 2018,

[8] A. E. Rad, M. S. M. Rahim, H. Kolivand, A. Norouzi, "Automatic computer-aided caries detection from dental x-ray images using intelligent level set", *Multimed Tools Appl*, Vol. 77, pp. 28843-28862, 2018.

[9] S. Salimzadeh and S. Kandulu, "Teeth Segmentation of Bitewing X-Ray Images Using Wavelet Transform", *Informatica*, Vol. 44, pp. 421-426, 2020.

[10] S. Datta and N. Chaki, "Dental X-ray image segmentation using Marker Based Watershed technique in Neutrosophic Domain", In: *Proc. of International Conference on Computer Science Engineering and Applications*, pp. 1-5, 2020.

[11] S. Tikhe, A. Naik, S. Bhide, T. Saravanan, and K. Kaliyamurthie, "Algorithm to Identify

Enamel Caries and Interproximal Caries Using Dental Digital Radiographs", In: *Proc. of International Advanced Computing Conferenc*e, pp. 225-228, 2016.

[12] J. Mao, K. Wang, Y. Hu, W. Sheng, and Q. Feng, "GrabCut algorithm for dental X-ray images based on full threshold segmentation", *IET Image Processing*, Vol. 12, No. 12, pp. 2330-2335, 2018.

[13] V. Majanga and S. Virir, "Dental Images' Segmentation Using Threshold Connected Component Analysis", *Hindawi Computational Intelligence and Neuroscience*, Vol. 2021, Article ID 2921508, pp. 1-9, 2021.

[14] T. Wagner and H. G. Lipinski, "IJBlob: an Image J library for connected component analysis and shape analysis", *Journal of Open Research Software*, Vol. 1, No. 1, p. e6, 2013.

[15] V. Chandran, G. S. Nizar, and P. Simon, "Segmentation of dental radiograph images", In: *Proc. of the 1ird International Conference on Advanced Informatics for Computing Research*, pp. 1-5, 2019.

[16] F. P. Mahdi and S. Kobashi, "Quantum Particle Swarm Optimization for Multilevel Thresholding-Based Image Segmentation on Dental X-Ray Images", In: *Proc. of Joint 10th International Conference on Soft Computing and Intelligent Systems and 19th International Symposium on Advanced Intelligent Systems*, 2018, pp. 1148-1153.

[17] M. K. Alsmadi, "A hybrid fuzzy c-means and neutrosophic for jaw lesion segmentation", *Shams Engineering Journal*, Vol. 9, No. 4, pp. 697-706, 2018.

[18] H. D. Cheng and Y Guo, "A New Neutrosophic Approach to Image Thresholding", *New Mathematics and Natural Computation*, Vol. 04, No. 03, pp. 291-308, 2008.

[19] L. H. Son, T. M, and Tuan, "A cooperative semi-supervised fuzzy clustering framework for dental x-ray image segmentation", *Expert Systems with Applications*, Vol. 46, pp. 380-393, 2016.

[20] M. Ali, L. H. Sonb, M. Khanc, and N. T. Tung, "Segmentation of dental X-ray images in medical imaging using neutrosophic orthogonal matrices", *Expert Systems with Applications*, Vol. 91, pp. 434-441, 2018.

[21] T. T. Ngan, T. M. Tuan, L. H. Son, N. H. Minh, and N. Dey, "Decision making based on Fuzzy aggregation operators for medical diagnosis from Dental X-Ray images", *Journal of Medical Systems*, Vol. 40, No. 12, p. 280, 2016.

[22] L. H. Sona, T. M. Tuanb, H. Fujitac, N. Dey, A. S. Ashour, V. T. N. Ngocf, L. Q. Anhf, D. T. Chu, "Dental diagnosis from X-Ray images: An expert system based on fuzzy computing", *Biomedical Signal Processing and Control*, Vol. 39, pp. 64-73, 2018.

[23] A. Fariza, A. Z. Arifin, E. R. Astuti, and T. Kurita, "Segmenting Tooth Components in Dental X-Ray Images Using Gaussian Kernel-Based Conditional Spatial Fuzzy C-Means Clustering Algorithm", *International Journal of Intelligent Engineering and Systems*, Vol. 12, No. 3, pp. 108-117, 2019, doi: 10.22266/ijies2019.0630.12.

[24] A. Kumar, H. S. Bhadauria, and A. Singh, "A semi-supervised Otsu based hyperbolic tangent Gaussian Kernel Fuzzy C-Mean Clustering for dental radiographs segmentation", *Multimedia Tools Applications*, Vol. 79, pp. 2745-2768, 2020.

[25] M. M. Hasan, R. Hassan, and W. Ismail, "Automatic segmentation of jaw from panoramic dental x-ray images using gvf snakes", In: *Proc. of World Automatic Congress*, pp. 1-6, 2016.

[26] P. Wang, "Fuzzy Set Theory and Its Applications", *Shanghai, China: Shanghai Scientific & Technical*, 1983.

[27] A. E. Rad, M. M. Rahim, H. Kolivand, and I. B. M. Amin, "Morphological region-based initial contour algorithm for level set methods in image segmentation", *Multimedia Tools and Applications*, Vol. 76, pp. 2185-2201, 2017.

[28] A. R. Kumari, S. N. Rao, and P. R. Reddy, "A Novel Method for Dental Radiographs Contrast Enhancement for Efficient Diagnosis of Dental Diseases", *International Journal of Innovative Technology and Exploring Engineering*, Vol. 8, No. 4S2, pp. 394-399, 2019.

[29] R. K. Devi, A. Banumathi, and G. Ulaganathan, "An automated and hybrid method for cyst segmentation in DXR images", *Cluster Computing*, Vol. 22, pp. S12179-S12191, 2019.